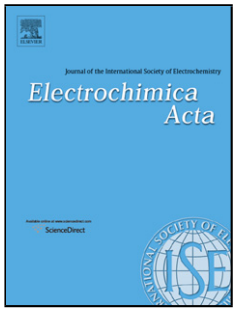

Title: Loading effect of carbon-supported platinum nanocubes on oxygen electroreduction

Authors: Kristel Jukk, Nadezda Kongi, Kaido Tammeveski, Rosa M. Arán-Ais, Jose Solla-Gullón, Juan M. Feliu

PII: S0013-4686(17)31740-1
DOI: http://dx.doi.org/10.1016/j.electacta.2017.08.099
Reference: EA 30103

To appear in: *Electrochimica Acta*

Received date: 9-5-2017
Revised date: 27-7-2017
Accepted date: 15-8-2017

Please cite this article as: Kristel Jukk, Nadezda Kongi, Kaido Tammeveski, Rosa M.Arán-Ais, Jose Solla-Gullón, Juan M.Feliu, Loading effect of carbon-supported platinum nanocubes on oxygen electroreduction, Electrochimica Actahttp://dx.doi.org/10.1016/j.electacta.2017.08.099

Loading effect of carbon-supported platinum nanocubes on oxygen electroreduction

Kristel Jukk[a], Nadezda Kongi[a], Kaido Tammeveski[a,1,*], Rosa M. Arán-Ais[b], Jose Solla-Gullón[b,1], Juan M. Feliu[b,1]

[a]*Institute of Chemistry, University of Tartu, Ravila 14a, 50411 Tartu, Estonia*

[b]*Instituto de Electroquímica, Universidad de Alicante, Apartado 99, 03080 Alicante, Spain*

Graphical abstract

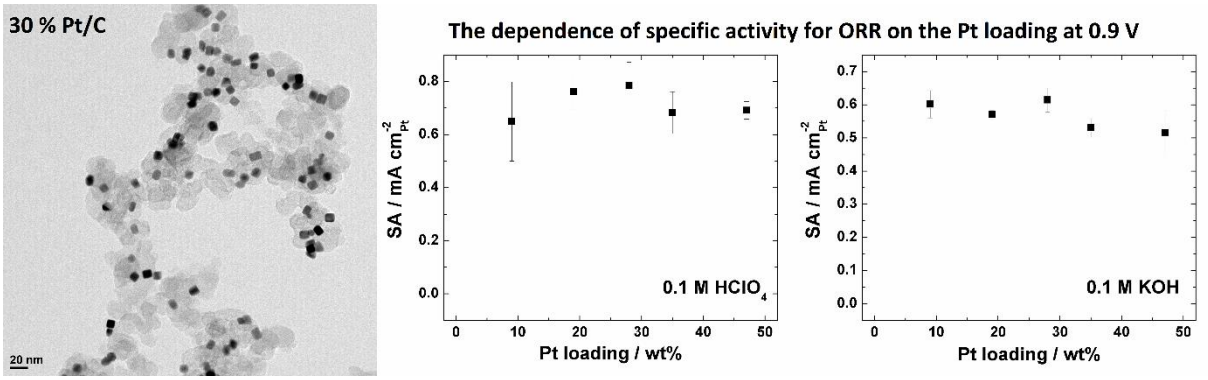

Research highlights

- Cubic Pt nanoparticles are synthesised in the presence of oleylamine and oleic acid
- Vulcan carbon is used as a support for cubic Pt nanoparticles with various loading
- Pt/C catalysts revealed a high ORR activity in both acid and alkaline solutions
- Pt/C catalysts showed similar specific and mass activity independently of Pt loading
- Important methodological aspects regarding Pt/C catalyst testing are highlighted

[*]Corresponding author. Tel.: +372 7375168; fax: +372 7375181.
E-mail address: kaido.tammeveski@ut.ee (K. Tammeveski).
[1]ISE member

Abstract

In this work, Vulcan carbon-supported cube-shape Pt nanoparticles with various metal loadings were synthesised in the presence of oleylamine and oleic acid. Surface morphology of different Pt/C samples was examined by transmission electron microscopy (TEM) and their metal loading verified by thermogravimetric analysis (TGA). TEM micrographs showed Pt nanoparticles with a preferential cubic-shape and increased agglomeration of the particles with increasing Pt loading. Electrochemical characterisation of the Pt/C catalysts indicated that the resulting Pt nanoparticles present a preferential (100) surface structure. The electrocatalytic properties of the Pt/C catalysts of different metal loading were evaluated towards the oxygen reduction reaction (ORR) both in acidic and alkaline media employing the rotating disk electrode (RDE) configuration. Interestingly, similar specific and mass activities were found in both solutions revealing that the ORR activities were independent of the Pt loading and suggesting that all the Pt nanocubes contributed as isolated particles.

***Keywords*:** Pt nanocubes; Shape-control; Carbon support; Electrocatalysis; Oxygen reduction

1. Introduction

Recent decades of research have shown that low-temperature fuel cells are promising and sustainable environmental-friendly power sources in the future [1-3]. Platinum-based catalysts show the highest electrocatalytic activity towards the oxygen reduction reaction (ORR) on the cathode of the low-temperature fuel cells [1, 3, 4]. Although platinum (Pt) is the best cathode catalyst for fuel cells [5, 6], it is still important to decrease the amount of this expensive and scarce noble metal in the platinum-based catalysts [4, 5]. On the other hand, particle size and catalyst surface structure are thought to be directly related to the electrocatalytic activity of Pt for ORR [7, 8]. In this regard, the control of the shape and composition is highly favourable to create new Pt-based nanostructures and to utilise scarce Pt more efficiently [9].

It has been established that the electroreduction of oxygen on single-crystal Pt surfaces is a structure-sensitive reaction [10]. The O_2 reduction studies on Pt(hkl) electrodes in aqueous 0.1 M $HClO_4$ and 0.1 M KOH solutions by Markovic et al. revealed that in alkaline media the ORR activity decreases in the following sequence (111) > (110) > (100), while in perchloric acid the variation in the O_2 reduction activities was found to be rather small between the three low-index facets, with activity increasing in the order (100) < (110) ≈ (111) [11-13]. Moreover, the order of the ORR activity on Pt(hkl) in sulphuric acid is completely different and decreases as follows: (110) > (100) > (111) [14]. It has been proposed that the differences in the activity in H_2SO_4 arise from stronger adsorption of the (bi)sulphate anions, which are considered as spectator species inhibiting the ORR process. On the stepped Pt surfaces it was found that the ORR activity in sulphuric and perchloric acid on Pt(111) was the lowest [15]. The O_2 reduction activity of Pt(110)-(1 × 1) was found to be lower than that of disordered Pt(110)-(1 × 2) in 0.1 M $HClO_4$ by 30-40 mV on the basis of the $E_{1/2}$ value [16].

The structure-sensitivity of the ORR process on Pt(hkl) low-index facets should lead to particle size effects according to the Kinoshita's cubo-octahedral model of Pt particles [17].

Several efforts have been made to understand the Pt particle size effect on the ORR kinetics [6, 18-28]. Mayrhofer et al. have reported in their early studies that the specific activity (SA) for O_2 reduction increases when the particle size increases [20, 21]. This activity change could be related to the higher Pt surface coverage by oxygen-containing species, which strongly block the active sites with decreasing Pt particle size. Sheng et al. studied the size-dependence of the ORR activity of Pt particles (size below 5 nm) on high-area carbon support in acidic electrolytes [22]. However, their results did not express any influence of the size on the specific and mass activities (MA) for O_2 reduction. Whilst the work by Sheng et al. revealed that the O_2 reduction activity was independent of the Pt particle size, it has been reported by Shao and co-workers that both SA and MA depend on the Pt particle size, if the particle diameter is under 10 nm [23]. These authors suggested that this behaviour is related to the oxygen binding energies on different Pt sites, which get accessible when the particle size changes. Furthermore, Shinozaki et al. [27], who varied the Pt particle diameter from 2 to 10 nm, showed that in 0.1 M $HClO_4$ solution the SA increased from 0.8 to 1.8 mA cm^{-2} with increasing particle size, and for particles bigger than 10 nm the activity plateaued to 2.7 mA cm^{-2} at 0.9 V vs RHE. It has been suggested by Mukerjee and McBreen that the decrease in the ORR electrocatalytic activity on smaller Pt particles (size below 5 nm) is related to the increase of Pt low-coordination sites on the surface of platinum nanoparticles, which inhibits the electroreduction of O_2 due to the strong adsorption of OH above 0.8 V vs RHE [19].

Conversely, several workgroups have studied Pt loading effect on the electrocatalytic activity for oxygen reduction [29-35]. Shih et al. varied the amount of the catalyst on the electrode surface [29], finding out that the SA was independent of the Pt loading on a carbon black support and it was considered to represent the intrinsic ORR activity of the catalyst. Quite similar results have been also reported by Higuchi et al., who changed the Pt loading level on carbon black from 19.2 to 63.2 wt% and found that the SA was almost constant for all the

catalysts studied [30]. Keeley and co-workers showed that by employing low and ultra-low Pt loadings in fuel cells, the catalytic activity did not depend on the amount of material used, however the stability diminished remarkably [31]. On the other hand, it was found by Schmidt and co-workers that by increasing the loading of Pt on the carbon support the SA for O_2 reduction increased, but MA decreased [32, 33]. These changes were caused by the transition from the state of isolated Pt nanoparticles to larger agglomerates. Strong correlation between the metal loading and the ORR activity was also shown by Speder et al. [34], when the Pt loading increased from 20 to 80 wt%, the SA increased from 470 to 775 μA cm^{-2} and MA values raised from 350 to 625 A g^{-1} in 0.1 M $HClO_4$ solution at 0.9 V vs RHE.

The uniform distribution of the catalyst on top of the glassy carbon (GC) electrode plays a critical role in the electroreduction of oxygen. Some research groups have aimed to prepare uniform catalyst coatings and understand the effect of even distribution on the reproducibility [36, 37]. Ke et al. used an in-house-developed automated electrode preparation device, which transferred ~3 nL droplets of the sonicated suspension of the Pt/C catalysts to controlled positions on the GC substrate [36]. This coating procedure resulted in higher diffusion-limited current values than inhomogeneous layers and these values were comparable to the theoretically calculated one. Also the reproducibility was much higher with the uniformly distributed catalyst layer. Another approach, which has been also used in the present research, was introduced by Garsany's group [37]. In that case, they dried the catalyst-modified GC electrodes by rotating at 700 rpm in order to obtain reproducible, smooth and thin electrocatalyst layers. They found that the specific and mass activities of platinum increased almost 56% and 72% compared to those prepared without electrode rotation while drying.

As aforementioned, the control over nanoparticles' shape is crucial in the ORR electrocatalytic activity. Although it was found that Pt(100) has the lowest activity compared to other Pt(hkl) single-crystal electrodes, several groups have studied oxygen reduction on

cubic Pt nanoparticles [28, 38-45]. Li et al. investigated the correlations between the surface morphology of Pt single-crystal and nanoparticles of varioust size and shape in perchloric acid [28]. They found that the initial ORR activity of 7-8 nm cubic, octahedral and cubo-octahedral nanoparticles is similar (~1 mA cm^{-2} at 0.9 V) and after some potential cycling the shape of Pt nanocubes and nanooctahedra converted to round-like polyhedral shape resulting in decreased ORR activities. Wang and co-workers prepared cubic-shaped, truncated cubic and polyhedral Pt nanoparticles (sizes varied from 3 to 7 nm) as electrocatalysts for O_2 reduction [39]. The obtained results showed an enhanced electrocatalytic activity of Pt nanocubes compared to other shapes, which confirmed that the shape-control of metal nanoparticle is important. In the previous work by the same group, Pt nanocubes were supported on carbon paper and they found that the SA of the supported Pt nanocubes was about 2-times higher than that of commercial Pt/C catalyst [40]. Fu et al. used a hydrothermal approach for synthesising monodisperse cubic Pt nanoparticles [42]. The as-prepared 6 nm Pt nanocubes exhibited highest SA and MA for ORR compared to commercially available Pt/C. Enhanced activity and stability was attributed to the combination of electronic and facet effects. Therefore, the use of shape-controlled Pt nanocrystals supported on carbon material has shown to be a promising approach to efficiently utilise the Pt for fuel cell applications.

Nonetheless, to our knowledge there is no report on the loading effect of cubic-shaped Pt nanoparticles supported on high-area nanocarbon material on the ORR kinetics. In this sense, it is worth noting that in order to properly evaluate the Pt loading effect i.e. the interparticle distance, the other physical parameters of the nanoparticles, particularly size, shape and surface structure should remain invariable for all catalyst samples and independently of their particular metal loading. The unique way of fulfilling these requirements is preparing all samples containing different metal loading from a single synthesis batch. A similar strategy has been previously used to study the effect of the metal loading towards other relevant

electrocatalytic reactions such as ammonia and formic acid electrooxidation for which the metal loading was shown to importantly affect the resulting electrocatalytic activity [46].

In the work reported in this paper, the loading effect of Vulcan carbon-supported Pt nanocubes (Pt/C) on the ORR kinetics in alkaline and acid solutions has been systematically investigated using a rotating disk electrode. Pt/C catalysts were characterised by transmission electron microscopy (TEM), the real Pt loading was found by thermogravimetric analysis (TGA) and for electrochemical characterisation CO-stripping and cyclic voltammetry (CV) experiments were conducted.

2. Experimental

2.1. Reagents

Platinum(II) acetylacetonate ($Pt(acac)_2$, 97%), oleylamine (OLA, 70%), oleic acid (OA, 90%) and tungsten hexacarbonyl ($W(CO)_6$, 99.99%) were purchased from Sigma-Aldrich. Sodium hydroxide (NaOH, p.a.) and potassium hydroxide (KOH, p.a.) were obtained from Merck. Methanol, ethanol and acetone (Reag. Ph. Eur) were purchased from Panreac, and n-hexane (96%) from Scharlau. All the chemicals of commercial origin were used without purification.

2.2. Synthesis of Pt nanocubes supported on Vulcan carbon

Cubic Pt nanoparticles were synthesised using a procedure previously reported [47,48]. The original synthesis procedure was scaled up by a factor of 6 so as to obtain a larger amount of the product, since it was important to prepare all loadings of Pt/C from a single batch. Briefly, 0.12 g of $Pt(acac)_2$, 48 mL of OLA and 12 mL of OA were added into a 3-necked flask and heated up to 130 ºC under argon atmosphere, while stirring at 500 rpm. At this temperature, 0.3 g of $W(CO)_6$ was added to the reaction mixture, followed by raising the temperature to 240 ºC for 30 min at 200 rpm. When the reaction entirely completed, the black dispersion was

immediately cooled down to room temperature and the Pt nanoparticles were then collected by applying centrifugation at 6000 rpm for 10 min. After pouring away the supernatant, the residue was re-suspended into 50 mL of hexane. For the preparation of Pt/C catalyst materials, the amount of carbon and Pt was calculated to obtain 35 mg of carbon-supported Pt catalyst. Thus, the suitable amount of nanoparticles suspension was mixed with the proper mass of Vulcan carbon to obtain the 10, 20, 30, 40 and 50 wt% Pt/C catalysts. The samples were then magnetically stirred for 30 min. The as-prepared catalyst materials were then washed following a protocol described elsewhere [48]. First, the catalyst samples were rinsed twice with hexane-ethanol mixture. The precipitate was then re-dispersed in 20 mL of methanol and a small amount of NaOH was added to the suspension, which was sonicated for 10 min. After the catalyst precipitated, the solution of methanol was removed and the carbon-supported Pt nanoparticles were rinsed with acetone. This purification procedure was repeated three times at least and the catalyst particles were vacuum filtered and rinsed with ultrapure water and ethanol. Final products were dried in an oven in ambient air at 70-80 °C for 12 h.

2.3. Physical characterisation of Pt/C catalysts

For the characterisation of the morphology, mean size and Pt particles distribution over the carbon support, a transmission electron microscope (JEOL, JEM-2010) working at 200 kV was employed. The samples for TEM were prepared by dropping of an aliquot of the hexane suspension of the Pt/C catalysts onto a Formvar-coated Cu grid and allowing the solvent to dry in air at room temperature. Thermogravimetric analysis (TGA) was conducted using a Mettler-Toledo TGA/SDTA851 thermobalance in order to experimentally determine the Pt loading (% in weight) of the prepared carbon-supported Pt nanocubes. The experiments were carried out in an oxidative atmosphere, N_2:O_2 with the ratio of 4:1 raising the temperature from 25 to 850 °C at a heating rate of 10 °C min^{-1}.

2.4. Electrochemical characterisation of Pt/C catalysts

Electrochemical measurements were conducted in a conventional three-electrode glass cell, where glassy carbon (GC) electrode coated with Pt/C catalysts was employed as working electrode, reversible hydrogen electrode (RHE) as reference electrode and a Pt wire as counter electrode. Autolab potentiostat/galvanostat PGSTAT302N and PGSTAT128N (Metrohm-Autolab B.V., The Netherlands) controlled with General Purpose Electrochemical System (GPES) software were used to record cyclic voltammograms (CV), CO electrooxidation and O_2 reduction polarisation curves. Also, in some cases, a VMP3 multichannel potentiostat (BioLogic) was employed, these measurements were conducted using the *NStat* configuration mode in which 6 GC rods (diameter 3 mm) as working electrodes were employed at the same time using the same reference and counter electrodes. The counter electrode was again a Pt wire and the RHE reference electrode was connected to the electrochemical cell via Luggin capillary.

Previous to any electrochemical experiment, the GC disks (geometric area of 0.071 cm^2) were polished on 0.3 μm alumina slurry (Buehler) for 3 min. After a thorough polishing, the GC disk electrode was rinsed and sonicated in Milli-Q water for 5 min. All Pt/C catalyst inks were prepared by dispersing 5 mg of the catalyst in 3.99 mL of Milli-Q water, 1 mL of isopropanol and 10 μL of Nafion (10 wt%, Sigma-Aldrich) and sonicating for 15 min. The working electrode was prepared by drop-coating 3 μL of the catalyst ink suspension onto the GC substrate. The GC electrodes coated with Pt/C catalysts were dried according to the procedure by Garsany et al. in Ar gas flow at 500 rpm at room temperature to obtain reproducible deposits of catalyst layer [37]. The Pt loadings on the modified GC electrode were 3.8, 8.0, 11.8, 14.8 and 19.9 $\mu g_{Pt}\ cm^{-2}$ for 10, 20, 30, 40 and 50 wt.% Pt/C catalysts, respectively.

Electrolyte solutions were prepared using sulphuric acid (Suprapur®, Merck), perchloric acid (Aldrich), potassium hydroxide or sodium hydroxide (Merck) and Milli-Q water. The electrolyte solutions were saturated with oxygen (99.999% AGA) or argon (99.999% AGA).

As usual, CO-stripping experiments were employed as ultimate cleaning procedure of the nanostructured Pt-based catalysts. The experimental details of CO adsorption and electrooxidation can be found in previous contributions [48-50]. The real electroactive area (A_r) of Pt nanocubes was estimated by employing charge integration in the hydrogen underpotential deposition (H_{UPD}) region (between 0.05 and 0.45 V) both in sulphuric and perchloric acid solutions after the correction for the electric double layer charging current and taking into account a total charge of 210 μC cm^{-2} for the adsorbed hydrogen monolayer [49].

The electroreduction of oxygen on the Pt/C catalysts was explored in O_2-saturated 0.1 M $HClO_4$ and 0.1 M KOH solutions using the rotating disk electrode (RDE) configuration at a scan rate (ν) of 10 mV s^{-1} in the potential range of 0.05–1.0 V. The RDE tests were carried out at the following electrode rotation rates (ω): 360; 610; 960; 1900; 3100 and 4600 rpm. A CTV101 speed control equipment and an EDI101 rotator (Radiometer, Copenhagen) were employed for the RDE testing of Pt/C catalysts. The background currents were also recorded at 10 mV s^{-1} between 0.05 and 1.0 V in Ar-saturated electrolyte solution and were subtracted from the experimental ORR current. All the electrochemical studies were conducted at room temperature (23±1 °C).

3. Results and discussion

3.1. TEM and TG characterisation of Pt/C samples

Figure 1 displays the characteristic TEM images for all the catalysts prepared in this work. Well-defined cubic-shaped Pt nanoparticles can be observed. As can be seen from Figure 1b-f, Pt nanocubes are rather evenly distributed on the surface of high-area Vulcan carbon

support and at higher Pt content more agglomerates are visible in the sample. For lower Pt content the nanoparticles are better separated from each other. Even though in this work the Pt nanocubes originate from the same synthesis batch, the estimation of their average particle size was done for each sample by measuring about 150-200 individual particles. The mean Pt particle sizes obtained were 9.25±1.24, 9.56±1.16, 9.63±1.11, 9.71±1.31, 9.44±1.16 and 9.29±0.9 nm corresponding to the unsupported Pt nanocubes and carbon supported with a nominal loading of 10, 20, 30, 40 and 50 wt%, respectively. As expected, within experimental error, the Pt nanocubes have the same mean particle size.

TG analyses were also carried out to estimate the real Pt content in electrocatalyst samples. The Pt content in carbon-supported catalysts was found to be 9, 19, 28, 35 and 47 wt% for nominal 10, 20, 30, 40 and 50 wt% Pt/C catalysts, respectively. The TGA results showed good correlations with the expected values from the experimental synthesis.

3.2. Surface structure characterisation by voltammetric measurements

It is well-recognised that, for Pt surfaces including massive and nanoparticulate electrodes, the cyclic voltammetric response in Ar-saturated 0.5 M H_2SO_4 and particularly the so-called hydrogen adsorption/desorption region can be used as fingerprint of the surface structure of the Pt electrode under study [51]. The voltammetric response of the catalyst samples here obtained is reported in Figure 2. As expected, the voltammetric profiles are essentially similar despite the different electric double layer charging contribution. Figure 2A shows the CV response for the unsupported Pt nanoparticles where the voltammetric features at about 0.12, 0.27 and 0.37 V vs RHE are characteristic to (110) sites, (100) steps and terrace borders and (100) terraces, respectively. Similar voltammetric responses have been obtained with analogous Pt nanocubes prepared using other synthetic routes [46, 48, 51] and denote the existence of a (100) predominant surface structure. Figure 2B reports the voltammetric

responses of the samples having different metal loading. For samples with lower Pt loadings (10 and 20 wt%), the double layer contribution is well-marked and is apparently related to the presence of the Vulcan carbon XC-72R catalyst support. Interestingly and regardless of the metal loading, the voltammetric responses of the different Pt/C catalyst samples are basically identical. However, it is worth noting that, in comparison with the unsupported samples (Figure 2A), all voltammetric features and particularly the feature at 0.37 V vs RHE characteristic to the presence of (100) terraces, are less defined/marked. This fact can be attributed to the Nafion used during the preparation of the inks [52], which is missing in the case of the pure (unsupported) Pt nanocubes which are simply dispersed in ultrapure water.

On the other hand, and taking into consideration that i) all Pt/C inks were prepared using the same total amount of catalyst (5 mg) and ii) the catalyst-modified GC electrodes were prepared by depositing the same volume of different inks (3 μL), the correct proportionality of the Pt electrochemically accessible surface area (A_r) of the Pt nanoparticles is warranted, particularly for high metal loading where an evident agglomeration of the Pt nanoparticles takes place (see Figure 1F). As described in previous contributions [46, 50], to estimate if the agglomeration of Pt nanoparticles induces a loss of the electroactive surface area, two analyses can be carried out, a) plotting the estimated A_r versus the corresponding metal loading (experimentally measured by TG analyses) and b) measuring the current ratio at 0.27 and 0.44 V vs RHE in the absence of any double layer charging correction and plotting this ratio versus the corresponding Pt loading. In both cases, as discussed in previous works [46, 50], a linear relationship should be observed. Figures 3A and 3B show the results obtained, respectively, and a good linear relationship is found in both cases, thus pointing out that the Vulcan carbon-supported Pt nanocubes were electrochemically accessible independently of the particular Pt loading and allowing the effect of the metal loading on the ORR rate to be properly studied both in acidic and alkaline media.

In order to precisely evaluate the specific surface area (SSA) of the catalyst samples their A_r was normalised to the corresponding mass of platinum. The Pt mass of each catalyst sample was calculated from the total mass of sample used in the experiment (3 μL of a 1 mg mL^{-1} suspension) and its particular Pt loading. The value of SSA was found to be constant for all the catalysts studied, which confirms that all the Pt nanocubes supported on Vulcan carbon are fully accessible as independent particles also in the agglomerates that were formed when the Pt content increased.

3.3. Oxygen reduction in 0.1 M $HClO_4$ and 0.1 M KOH solutions

The electroreduction of O_2 was first studied in acidic media (0.1 M $HClO_4$). Figures 4A and 4B show the voltammetric response of the different samples in Ar-saturated 0.1 M $HClO_4$ solution. Similarly to the CV results obtained in 0.5 M H_2SO_4, the voltammetric profiles of the carbon supported samples (Figure 4B) are similar to that obtained with the pure Pt nanocubes (Figure 4A). As discussed in previous contributions [53], the voltammetric profile displays characteristic contributions, between 0.3-0.5 V, related to the OH adsorption on the (100) well-ordered domains whereas, the contributions in the range between 0.09-0.22 V can be attributed to (110) sites. In addition, as shown in Figure 4C, a linear relationship is again found between the A_r and the specific metal loading of the samples.

The positive-going sweeps at different rotation speeds of the ORR polarisation curves for 30% Pt/C catalyst are presented in Figure 5A. For all electrode rotation rates, single-waved current density-potential (*j*-*E*) curves with diffusion-limited current plateaus were observed.

To get more insight into the O_2 reduction process on Pt/C catalysts, the obtained ORR data was further analysed using the Koutecky-Levich (K-L) equation:

$$\frac{1}{j} = \frac{1}{j_k} + \frac{1}{j_d} = -\frac{1}{nFkC_{O_2}^b} - \frac{1}{0.62nFD_{O_2}^{2/3}\nu^{-1/6}C_{O_2}^b\omega^{1/2}} \quad (1)$$

where j is the experimentally measured O_2 reduction current density at a specific potential E, j_k is the kinetically controlled current density at E and j_d is the diffusionally controlled current density, n is the electron transfer number, k is the electrochemical rate constant for ORR at a specific potential E (cm s^{-1}), F is the Faraday constant (96485 C mol^{-1}), ω is the rotation rate of the electrode (rad s^{-1}), $C_{O_2}^b$ is the concentration of O_2 in the bulk solution (1.26×10^{-6} mol cm^{-3}) [54], D_{O_2} is the diffusion coefficient of O_2 (1.93×10^{-5} cm^2 s^{-1}) [54] and v is the kinematic viscosity of the electrolyte solution (0.01 cm^2 s^{-1}) [55]. These $C_{O_2}^b$ and D_{O_2} values are given for 0.1 M $HClO_4$ solution. Linear and parallel Koutecky-Levich plots are shown in Figure 5B. The K-L analysis revealed that the electron transfer number was close to 4 for all the catalyst materials tested (inset to Figure 5B), indicating that O_2 is fully reduced to water. Similar n values have been reported for various Pt-based catalysts in the literature [56-61].

Figure 5C shows some representative anodic sweeps of the oxygen reduction polarisation curves for the different Pt/C catalysts in O_2-saturated 0.1 M $HClO_4$ solution recorded at a rotation speed of 1900 rpm. It can be observed that with increasing Pt loading, the ORR onset potential (E_{onset}) and half-wave potential ($E_{1/2}$) shift towards positive values. The E_{onset} is 0.93 and 0.99 V for 10% Pt/C and 50% Pt/C catalysts, respectively. The $E_{1/2}$ value for 10% Pt/C is 0.74 V and it increases to 0.85 V for 50% Pt/C catalyst. Similar tendency has been also found by Fabbri et al. [32, 33]. The $E_{1/2}$ values for all the Pt/C catalysts are summarised in Table 1. Similar E_{onset} and $E_{1/2}$ values have been also reported by Kim et al., who studied oxygen reduction on polycrystalline Pt nanoparticles supported on ordered mesoporous carbon [62].

Tafel plots for O_2 reduction shown in Figure 5D were obtained from the RDE data at 1900 rpm. Two specific Tafel regions with distinct slopes were observed. At low overpotentials the slope was close to -60 mV and at high overpotentials it increased to -120 mV. Similar Tafel behaviour for O_2 reduction in perchloric acid has been reported in earlier works [57, 58, 63].

Specific activities (SA) for O_2 reduction on Pt/C catalysts at 0.9 V were calculated as follows:

$$SA = I_k / A_r \quad (2)$$

where I_k is the kinetic current at a given potential and A_r is the real electroactive area of Pt.

The kinetic currents I_k at 0.9 V were obtained from the ORR polarisation curves by considering the Koutecky-Levich equation:

$$\frac{1}{I} = \frac{1}{I_k} + \frac{1}{I_d} \rightarrow I_k = \frac{I_d \times I}{I_d - I} \quad (3)$$

where I is the current measured at 0.9 V, I_k is the kinetic current and I_d is the diffusion-limited current. It is worth noting that the reported SA values are mean values calculated at least from 3-4 independent and statistically significant ORR measurements. At this respect, it is important to recall that the ORR activity and reproducibility are strongly affected by a number of experimental parameters [64,65] that control the catalyst film thickness and uniformity (film quality). The lack of control of these experimental parameters is the origin of inaccurate, irreproducible and unreliable ORR measurements [64,65].

Figure 6A reports the SA values obtained with the different samples. As can be seen, the value of SA is almost constant for all the catalysts studied (0.71±0.07 mA cm^{-2}), which is in accordance with our assumptions that the reaction kinetics are identical and does not depend on the Pt loading. Compared to some other studies [22, 42, 59] the SA values found in this work are approximately two to three times higher, but the differences may arise from the Pt particle size, as described in the respective literature, the SA value increases with increasing the particle size.

Mass activity (MA) for O_2 reduction of each electrode was evaluated using the following equation:

$$MA = I_k / m_{Pt} \quad (4)$$

where m_{Pt} is the mass of Pt, which was calculated using the concentration of the catalyst ink (1 mg mL^{-1}), volume deposited onto the GC electrode (3 µL) and Pt loading determined by TGA. As previously stated for the SA values, the MA values are mean values obtained from

at least 3-4 independent measurements. The mass activities vs. Pt loading are shown in Figure 6B. The average MA at 0.9 V was found to be 59.2±5.9 mA mg^{-1}. Almost constant MA value for all the Pt/C catalysts studied indicates that the mass activity does not depend on the loading of Pt nanocubes. The observed MA values are somewhat smaller than that found for smaller Pt particles in the literature [22, 23, 66, 67]. It has been suggested in earlier studies that Pt particles in the size range of 3.3-3.5 nm show the highest MA values [17, 68, 69]. Comparable MA for O_2 reduction have been reported by Kim et al. for ~1 nm Pt nanoparticles supported on ordered mesoporous carbons [62] and by Angelopoulos and co-workers on clustered and single crystal Pt nanoparticles [70].

The oxygen reduction studies were also carried out in O_2-saturated 0.1 M KOH solution. Figure 7A reports the voltammetric response of the different samples in Ar-saturated 0.1 M KOH solution. As expected, the voltammetric profile of the samples shows different contributions which are well-established to be associated with a (100) preferential surface structure [53]. In alkaline solution, the calculation of the A_r values is not as well-defined as in acidic solution (H_2SO_4 and $HClO_4$). In this regard a reference value of 390 μC cm^{-2} for the total charge density measured between 0.06 and 0.90 V (without any double-layer correction) was proposed [53]. Unfortunately, this calculation is only valid for pure Pt nanoparticles but not for carbon-supported Pt nanoparticles due to a significant contribution of the carbon support to the electric double layer region. In this work, we proposed a different approach which involves the calculation of the charge between 0.05 and 0.65 V after double-layer correction as visually described in Figure 7B. The double layer contribution is estimated from the current at 0.65 V and a charge density value of 187 μC cm^{-2} is used. This charge density value is an average value deduced from the charge density values of 282, 164 and 114 μC cm^{-2} corresponding to Pt(100), Pt(110) and Pt(111) single crystal electrodes, respectively [71]. Interestingly, the calculated surface areas are essentially similar to those obtained in 0.1

M $HClO_4$ (Table 1) and also show a linear relationship with the Pt loading (Figure 7C). These facts further confirm the validity of our approach.

Figure 8A presents the positive-going ORR polarisation curves for 30% Pt/C catalyst. The *j-E* curves for all the electrodes tested in alkaline media were also single-waved with well-defined diffusion-limited current plateaus as observed in acidic electrolyte. The RDE polarisation data recorded in alkaline solution were treated using Eq. (1), where the values of O_2 diffusion coefficient (D_{O_2}=1.9×10^{-5} cm^2 s^{-1} [72]) and solubility ($C_{O_2}^b$=1.2×10^{-6} mol cm^{-3} [72]) were used for 0.1 M KOH solution. The obtained K–L plots (Figure 8B) were linear and parallel, revealing the first order kinetics towards O_2 concentration and similar *n* values at various electrode potentials. From the slope of the K–L plots the value of *n* was found to be close to four for each electrode (inset to Figure 8B). The four-electron O_2 reduction pathway on Pt-based catalysts in alkaline media has been reported previously [60, 73-77].

Figure 8C displays a comparison of the RDE results at 1900 rpm. As in acid media, the values of E_{onset} and $E_{1/2}$ for O_2 electroreduction on Pt/C catalysts in alkaline media are more positive when the amount of Pt in the catalysts increases. The E_{onset} for 50% Pt/C is 0.99 V and it decreases to 0.94 V for 10% Pt/C. The $E_{1/2}$ values obtained in alkaline solution for all the Pt/C catalysts studied are listed in Table 1. The highest $E_{1/2}$ value of 0.85 V was found for 50% Pt/C. It has been reported by Markovic et al. that Pt(100) single-crystal electrode shows higher electrocatalytic activity for ORR in 0.1 M $HClO_4$ solution as compared to 0.1 M KOH [13]. In our work, the activity of O_2 reduction is enhanced in alkaline media, the reason of which needs further investigation.

Tafel plots for O_2 reduction on Pt/C catalysts materials in 0.1 M KOH solution are shown in Figure 8D. Two regions of different Tafel slope were found. At low overpotentials the slope values for Pt nanocatalysts were around -60 mV and in the second Tafel region the slope

values were close to -120 mV [73, 75-77]. The change in the Tafel slope is related to the potential-dependent coverage of oxygenated species on the surface of Pt catalysts.

The SA values for O_2 reduction on the Pt/C catalysts in alkaline media were calculated also at 0.9 V vs RHE and are presented in Figure 9A. In 0.1 M KOH solution all the Pt/C catalysts showed almost constant SA. The average value of SA was around 0.57±0.04 mA cm^{-2}. The SA value for 10% Pt/C catalyst was slightly higher than that of other Pt loadings. This observation might arise also from the errors in calculating the electroactive area of Pt by integrating the charge under the hydrogen desorption peaks. The SA values in both solutions were rather similar, which may be due to a relatively weak adsorption of spectator species in these electrolytes ($HClO_4$ and KOH). It is quite obvious that the O_2 reduction kinetics is largely influences by the coverage of adsorbed OH on Pt in these electrolytes, which decreases the ORR rate.

The mass activity in 0.1 M KOH showed almost constant values for O_2 reduction on all the catalysts studied (Figure 9B). The mean value of MA for the carbon-supported Pt/C materials was 53.1±3.4 mA mg^{-1} at 0.9 V, which is slightly lower than that found in acidic media.

The effect of Pt particle size in ORR electrocatalysis has been a matter of controversy [78]. According to several previous studies the size effect of platinum particles on the ORR kinetics has been reported for smaller nanoparticles than 6-7 nm [28]. Above this particle diameter the SA is virtually constant. The investigation of Pt particle size effect in different electrolytes did not yield the expected results on the basis of model predictions of cubo-octahedral Pt particles [79]. The size of Pt nanocubes studied in the present work is above the size range for which the change in the SA value is expected. Also, there have been variations regarding the ORR activity trend of shape-controlled Pt nanoparticles, which might arise from imperfect particle shapes. Even though the overall quality of particle shape could be perfect in some studies on the basis of HR-TEM images, there is still a high likelihood that Pt surface atoms of lower

coordination number exist and this could lead to scatter in the data and differences in the electrocatalytic ORR behaviour. At this respect, the synthesis and ORR activity of well-defined 3-4 nm Pt nanocubes is still a challenge and would represent a significant advance because it would perfectly fulfil with the requirement to be applied in practical devices. Unfortunately, decreasing Pt particle size tends to decrease the quality of the shaped nanoparticles, in terms of surface domains with preferential surface structure, and increase the presence of low-coordination surface sites such as steps, kinks and corners.

4. Conclusions

Pt nanocubes were synthesised via oleylamine/oleic acid method and supported on the high-area carbon. Nanocatalysts were characterised by transmission electron microscopy. TEM micrographs showed that cubic-shaped Pt nanoparticles were uniformly distributed on the carbon support. Cyclic voltammetry experiments showed characteristic hydrogen adsorption/desorption peaks of Pt(100) facets in all three electrolytes studied. The RDE measurements showed increased overall ORR electrocatalytic activity with increasing Pt content in the catalyst. The specific and mass activities were found to be constant for all the Pt loadings studied, indicating that these are independent of the amount of Pt dispersed on the carbon support. The Tafel analysis revealed that in both solutions the O_2 reduction mechanism was the same for all the catalyst materials and the rate-determining step is the slow transfer of the first electron to O_2 molecule.

Acknowledgements

This work was financially supported by institutional research funding (IUT20-16) of the Estonian Ministry of Education and Research. This research was also supported by the EU through the European Regional Development Fund (TK141 “Advanced materials and high-

technology devices for energy recuperation systems"). KJ would like to thank Archimedes Foundation for the partial study scholarship. JMF thanks MINECO (Project CTQ2016-76221-P (AEI/FEDER, UE)) and Generalitat Valenciana (Project PROMETEOII/2014/013) for financial support. JSG acknowledges financial support from VITC (Vicerrectorado de Investigación y Transferencia de Conocimiento) of the University of Alicante.

References

[1] H.A. Gasteiger, S.S. Kocha, B. Sompalli, F.T. Wagner, Activity benchmarks and requirements for Pt, Pt-alloy, and non-Pt oxygen reduction catalysts for PEMFCs, Applied Catalysis B: Environmental 56(1–2) (2005) 9-35.

[2] S. Sharma, B.G. Pollet, Support materials for PEMFC and DMFC electrocatalysts - A review, Journal of Power Sources 208 (2012) 96-119.

[3] S.S. Zhang, X.Z. Yuan, J.N.C. Hin, H.J. Wang, K.A. Friedrich, M. Schulze, A review of platinum-based catalyst layer degradation in proton exchange membrane fuel cells, Journal of Power Sources 194(2) (2009) 588-600.

[4] Y. Nie, L. Li, Z.D. Wei, Recent advancements in Pt and Pt-free catalysts for oxygen reduction reaction, Chemical Society Reviews 44(8) (2015) 2168-2201.

[5] H.F. Lv, D.G. Li, D. Strmcnik, A.P. Paulikas, N.M. Markovic, V.R. Stamenkovic, Recent advances in the design of tailored nanomaterials for efficient oxygen reduction reaction, Nano Energy 29 (2016) 149-165.

[6] E. Antolini, Structural parameters of supported fuel cell catalysts: The effect of particle size, inter-particle distance and metal loading on catalytic activity and fuel cell performance, Applied Catalysis B-Environmental 181 (2016) 298-313.

[7] M. Nesselberger, M. Roefzaad, R.F. Hamou, P.U. Biedermann, F.F. Schweinberger, S. Kunz, K. Schloegl, G.K.H. Wiberg, S. Ashton, U. Heiz, K.J.J. Mayrhofer, M. Arenz, The

effect of particle proximity on the oxygen reduction rate of size-selected platinum clusters, Nature Materials 12(10) (2013) 919-924.

[8] J.B. Wu, H. Yang, Platinum-based oxygen reduction electrocatalysts, Accounts of Chemical Research 46(8) (2013) 1848-1857.

[9] M.T.M. Koper, Structure sensitivity and nanoscale effects in electrocatalysis, Nanoscale 3(5) (2011) 2054-2073.

[10] N.M. Markovic, P.N. Ross, Surface science studies of model fuel cell electrocatalysts, Surface Science Reports 45(4-6) (2002) 121-229.

[11] N.M. Markovic, R.R. Adzic, B.D. Cahan, E.B. Yeager, Structural effects in electrocatalysis - oxygen reduction on platinum low-index single-crystal surfaces in perchloric-acid solutions, Journal of Electroanalytical Chemistry 377(1-2) (1994) 249-259.

[12] N.M. Markovic, H.A. Gasteiger, P.N. Ross, Oxygen reduction on platinum low-index single-crystal surfaces in alkaline solution: Rotating ring disk(Pt(hkl)) studies, Journal of Physical Chemistry 100(16) (1996) 6715-6721.

[13] N. Markovic, H. Gasteiger, P.N. Ross, Kinetics of oxygen reduction on Pt(hkl) electrodes: Implications for the crystallite size effect with supported Pt electrocatalysts, Journal of the Electrochemical Society 144(5) (1997) 1591-1597.

[14] N.M. Markovic, H.A. Gasteiger, P.N. Ross, Oxygen reduction on platinum low-index single-crystal surfaces in sulfuric acid solution: Rotating ring-Pt(hkl) disk studies, Journal of Physical Chemistry 99(11) (1995) 3411-3415.

[15] A. Kuzume, E. Herrero, J.M. Feliu, Oxygen reduction on stepped platinum surfaces in acidic media, Journal of Electroanalytical Chemistry 599(2) (2007) 333-343.

[16] G.A. Attard, A. Brew, Cyclic voltammetry and oxygen reduction activity of the Pt{110}-(1 x 1) surface, Journal of Electroanalytical Chemistry 747 (2015) 123-129.

[17] K. Kinoshita, Particle size effects for oxygen reduction on highly dispersed platinum in acid electrolytes, Journal of the Electrochemical Society 137(3) (1990) 845-848.

[18] A. Kabbabi, F. Gloaguen, F. Andolfatto, R. Durand, Particle-size effect for oxygen reduction and methanol oxidation on Pt/C inside a proton-exchange membrane, Journal of Electroanalytical Chemistry 373(1-2) (1994) 251-254.

[19] S. Mukerjee, J. McBreen, Effect of particle size on the electrocatalysis by carbon-supported Pt electrocatalysts: an in situ XAS investigation, Journal of Electroanalytical Chemistry 448(2) (1998) 163-171.

[20] K.J.J. Mayrhofer, B.B. Blizanac, M. Arenz, V.R. Stamenkovic, P.N. Ross, N.M. Markovic, The impact of geometric and surface electronic properties of Pt-catalysts on the particle size effect in electocatalysis, Journal of Physical Chemistry B 109(30) (2005) 14433-14440.

[21] K.J.J. Mayrhofer, D. Strmcnik, B.B. Blizanac, V. Stamenkovic, M. Arenz, N.M. Markovic, Measurement of oxygen reduction activities via the rotating disc electrode method: From Pt model surfaces to carbon-supported high surface area catalysts, Electrochimica Acta 53(7) (2008) 3181-3188.

[22] W.C. Sheng, S. Chen, E. Vescovo, Y. Shao-Horn, Size influence on the oxygen reduction reaction activity and instability of supported Pt nanoparticles, Journal of the Electrochemical Society 159(2) (2012) B96-B103.

[23] M. Shao, A. Peles, K. Shoemaker, Electrocatalysis on platinum nanoparticles: Particle size effect on oxygen reduction reaction activity, Nano Letters 11(9) (2011) 3714-3719.

[24] K. Yamamoto, T. Imaoka, W.J. Chun, O. Enoki, H. Katoh, M. Takenaga, A. Sonoi, Size-specific catalytic activity of platinum clusters enhances oxygen reduction reactions, Nature Chemistry 1(5) (2009) 397-402.

[25] S.J. Ashton, A. Novo, K.J. Mayrhofer, M. Arenz, Influence of the electrolyte on the particle size effect of the oxygen reduction reaction on Pt nanoparticles, ECS Transactions 25(1) (2009) 455-462.

[26] A. Anastasopoulos, J.C. Davies, L. Hannah, B.E. Hayden, C.E. Lee, C. Milhano, C. Mormiche, L. Offin, The particle size dependence of the oxygen reduction reaction for carbon-supported platinum and palladium, ChemSusChem 6(10) (2013) 1973-1982.

[27] K. Shinozaki, Y. Morimoto, B.S. Pivovar, S.S. Kocha, Re-examination of the Pt particle size effect on the oxygen reduction reaction for ultrathin uniform Pt/C catalyst layers without influence from Nafion, Electrochimica Acta 213 (2016) 783-790.

[28] D.G. Li, C. Wang, D.S. Strmcnik, D.V. Tripkovic, X.L. Sun, Y.J. Kang, M.F. Chi, J.D. Snyder, D. van der Vliet, Y.F. Tsai, V.R. Stamenkovic, S.H. Sun, N.M. Markovic, Functional links between Pt single crystal morphology and nanoparticles with different size and shape: the oxygen reduction reaction case, Energy & Environmental Science 7(12) (2014) 4061-4069.

[29] Y.H. Shih, G.V. Sagar, S.D. Lin, Effect of electrode Pt loading on the oxygen reduction reaction evaluated by rotating disk electrode and its implication on the reaction kinetics, Journal of Physical Chemistry C 112(1) (2008) 123-130.

[30] E. Higuchi, H. Uchida, M. Watanabe, Effect of loading level in platinum-dispersed carbon black electrocatalysts on oxygen reduction activity evaluated by rotating disk electrode, Journal of Electroanalytical Chemistry 583(1) (2005) 69-76.

[31] G.P. Keeley, S. Cherevko, K.J.J. Mayrhofer, The stability challenge on the pathway to low and ultra-low platinum loading for oxygen reduction in fuel cells, ChemElectroChem 3(1) (2016) 51-54.

[32] E. Fabbri, S. Taylor, A. Rabis, P. Levecque, O. Conrad, R. Kotz, T.J. Schmidt, The effect of platinum nanoparticle distribution on oxygen electroreduction activity and selectivity, ChemCatChem 6(5) (2014) 1410-1418.

[33] S. Taylor, E. Fabbri, P. Levecque, T.J. Schmidt, O. Conrad, The effect of platinum loading and surface morphology on oxygen reduction activity, Electrocatalysis 7(4) (2016) 287-296.

[34] J. Speder, I. Spanos, A. Zana, J.J.K. Kirkensgaard, K. Mortensen, L. Altmann, M. Baumer, M. Arenz, From single crystal model catalysts to systematic studies of supported nanoparticles, Surface Science 631 (2015) 278-284.

[35] A. Kriston, T.Y. Xie, P. Ganesan, B.N. Popov, Analysis of the effect of Pt loading on mass and specific activity in PEM fuel cells, Journal of the Electrochemical Society 160(4) (2013) F406-F412.

[36] K. Ke, K. Hiroshima, Y. Kamitaka, T. Hatanaka, Y. Morimoto, An accurate evaluation for the activity of nano-sized electrocatalysts by a thin-film rotating disk electrode: Oxygen reduction on Pt/C, Electrochimica Acta 72 (2012) 120-128.

[37] Y. Garsany, I.L. Singer, K.E. Swider-Lyons, Impact of film drying procedures on RDE characterization of Pt/VC electrocatalysts, Journal of Electroanalytical Chemistry 662(2) (2011) 396-406.

[38] M. Inaba, M. Ando, A. Hatanaka, A. Nomoto, K. Matsuzawa, A. Tasaka, T. Kinumoto, Y. Iriyama, Z. Ogumi, Controlled growth and shape formation of platinum nanoparticles and their electrochemical properties, Electrochimica Acta 52(4) (2006) 1632-1638.

[39] C. Wang, H. Daimon, T. Onodera, T. Koda, S. Sun, A general approach to the size- and shape-controlled synthesis of platinum nanoparticles and their catalytic reduction of oxygen, Angewandte Chemie-International Edition 47(19) (2008) 3588-3591.

[40] C. Wang, H. Daimon, Y. Lee, J. Kim, S. Sun, Synthesis of monodisperse Pt nanocubes and their enhanced catalysis for oxygen reduction, Journal of the American Chemical Society 129(22) (2007) 6974-6975.

[41] T. Yu, D.Y. Kim, H. Zhang, Y.N. Xia, Platinum concave nanocubes with high-index facets and their enhanced activity for oxygen reduction reaction, Angewandte Chemie-International Edition 50(12) (2011) 2773-2777.

[42] G.T. Fu, K. Wu, X. Jiang, L. Tao, Y. Chen, J. Lin, Y.M. Zhou, S.H. Wei, Y.W. Tang, T.H. Lu, X.H. Xia, Polyallylamine-directed green synthesis of platinum nanocubes. Shape and electronic effect codependent enhanced electrocatalytic activity, Physical Chemistry Chemical Physics 15(11) (2013) 3793-3802.

[43] B.Y. Xia, H.B. Wu, Y. Yan, H.B. Wang, X. Wang, One-pot synthesis of platinum nanocubes on reduced graphene oxide with enhanced electrocatalytic activity, Small 10(12) (2014) 2336-2339.

[44] R. Devivaraprasad, R. Ramesh, N. Naresh, T. Kar, R.K. Singh, M. Neergat, Oxygen reduction reaction and peroxide generation on shape-controlled and polycrystalline platinum nanoparticles in acidic and alkaline electrolytes, Langmuir 30(29) (2014) 8995-9006.

[45] V. Grozovski, H. Kasuk, J. Nerut, E. Härk, R. Jäger, I. Tallo, E. Lust, Oxygen reduction at shape-controlled platinum nanoparticles and composite catalysts based on (100)Pt nanocubes on microporous-mesoporous carbon supports, ChemElectroChem 2(6) (2015) 847-851.

[46] F.J. Vidal-Iglesias, V. Montiel, J. Solla-Gullón, Influence of the metal loading on the electrocatalytic activity of carbon-supported (100) Pt nanoparticles, Journal of Solid State Electrochemistry 20(4) (2016) 1107-1118.

[47] J. Zhang, J. Fang, A General strategy for preparation of Pt 3d-transition metal (Co, Fe, Ni) nanocubes, Journal of the American Chemical Society 131(51) (2009) 18543-18547.

[48] R.M. Aran-Ais, F.J. Vidal-Iglesias, J. Solla-Gullon, E. Herrero, J.M. Feliu, Electrochemical characterization of clean shape-controlled Pt nanoparticles prepared in presence of oleylamine/oleic acid, Electroanalysis 27(4) (2015) 945-956.

[49] J. Solla-Gullon, V. Montiel, A. Aldaz, J. Clavilier, Electrochemical characterisation of platinum nanoparticles prepared by microemulsion: how to clean them without loss of crystalline surface structure, Journal of Electroanalytical Chemistry 491 (2000) 69-77.

[50] A. Lopez-Cudero, J. Solla-Gullon, E. Herrero, A. Aldaz, J.M. Feliu, CO electrooxidation on carbon supported platinum nanoparticles: Effect of aggregation, Journal of Electroanalytical Chemistry 644(2) (2010) 117-126.

[51] J. Solla-Gullon, P. Rodriguez, E. Herrero, A. Aldaz, J.M. Feliu, Surface characterization of platinum electrodes, Physical Chemistry Chemical Physics 10(10) (2008) 1359-1373.

[52] M.S. McGovern, E.C. Garnett, C. Rice, R.I. Masel, A. Wieckowski, Effects of Nafion as a binding agent for unsupported nanoparticle catalysts, Journal of Power Sources 115 (2003) 35-39.

[53] F.J. Vidal-Iglesias, R.M. Arán-Ais, J. Solla-Gullón, E. Herrero, J.M. Feliu, Electrochemical characterization of shape-controlled Pt nanoparticles in different supporting electrolytes, ACS Catalysis 2(5) (2012) 901-910.

[54] R.R. Adzic, J. Wang, B.M. Ocko, Structure of metal adlayers during the course of electrocatalytic reactions: O_2 reduction on Au(111) with Tl adlayers in acid solutions, Electrochimica Acta 40(1) (1995) 83-89.

[55] D.R. Lide, CRC Handbook of Chemistry and Physics, 82nd ed., CRC Press, Boca Raton, 2001.

[56] T.J. Schmidt, U.A. Paulus, H.A. Gasteiger, R.J. Behm, The oxygen reduction reaction on a Pt/carbon fuel cell catalyst in the presence of chloride anions, Journal of Electroanalytical Chemistry 508(1-2) (2001) 41-47.

[57] A. Sarapuu, A. Kasikov, T. Laaksonen, K. Kontturi, K. Tammeveski, Electrochemical reduction of oxygen on thin-film Pt electrodes in acid solutions, Electrochimica Acta 53(20) (2008) 5873-5880.

[58] A. Sarapuu, S. Kallip, A. Kasikov, L. Matisen, K. Tammeveski, Electroreduction of oxygen on gold-supported thin Pt films in acid solutions, Journal of Electroanalytical Chemistry 624(1-2) (2008) 144-150.

[59] L. Borchardt, F. Hasche, M.R. Lohe, M. Oschatz, F. Schmidt, E. Kockrick, C. Ziegler, T. Lescouet, A. Bachmatiuk, B. Buchner, D. Farrusseng, P. Strasser, S. Kaskel, Transition metal loaded silicon carbide-derived carbons with enhanced catalytic properties, Carbon 50(5) (2012) 1861-1870.

[60] N. Gavrilov, M. Dasic-Tomic, I. Pasti, G. Ciric-Marjanovic, S. Mentus, Carbonized polyaniline nanotubes/nanosheets-supported Pt nanoparticles: Synthesis, characterization and electrocatalysis, Materials Letters 65(6) (2011) 962-965.

[61] C. Koenigsmann, W.P. Zhou, R.R. Adzic, E. Sutter, S.S. Wong, Size-dependent enhancement of electrocatalytic performance in relatively defect-free, processed ultrathin platinum nanowires, Nano Letters 10(8) (2010) 2806-2811.

[62] N.I. Kim, J.Y. Cheon, J.H. Kim, J. Seong, J.Y. Park, S.H. Joo, K. Kwon, Impact of framework structure of ordered mesoporous carbons on the performance of supported Pt catalysts for oxygen reduction reaction, Carbon 72 (2014) 354-364.

[63] A. Damjanovic, V. Brusic, Electrode kinetics of oxygen reduction on oxide-free platinum electrodes, Electrochimica Acta 12(6) (1967) 615-628.

[64] I.A. Safo, M. Oezaslan, Electrochemical cleaning of polyvinylpyrrolidone-capped Pt nanocubes for the oxygen reduction reaction, Electrochimica Acta 241 (2017) 544-552.

[65] S.S. Kocha, K. Shinozaki, J.W. Zack, D.J. Myers, N.N. Kariuki, T. Nowicki, V. Stamenkovic, Y. Kang, D. Li, D. Papageorgopoulos, Best practices and testing protocols for bencmarking ORR activities of fuel cell electrocatalysts using rotating disk electrode, Electrocatalysis 8(4) (2017) 366-374.

[66] S.H. Joo, K. Kwon, D.J. You, C. Pak, H. Chang, J.M. Kim, Preparation of high loading Pt nanoparticles on ordered mesoporous carbon with a controlled Pt size and its effects on oxygen reduction and methanol oxidation reactions, Electrochimica Acta 54(24) (2009) 5746-5753.

[67] F.J. Perez-Alonso, D.N. McCarthy, A. Nierhoff, P. Hernandez-Fernandez, C. Strebel, I.E.L. Stephens, J.H. Nielsen, I. Chorkendorff, The effect of size on the oxygen electroreduction activity of mass-selected platinum nanoparticles, Angewandte Chemie-International Edition 51(19) (2012) 4641-4643.

[68] M.L. Sattler, P.N. Ross, The surface-structure of Pt crystallites supported on carbon-black, Ultramicroscopy 20(1-2) (1986) 21-28.

[69] F. Maillard, S. Pronkin, E.R. Savinova, Influence of size on the electrocatalytic activities of supported metal nanoparticles in fuel cells related reactions, in: W. Vielstich, H.A. Gasteiger, H. Yokokawa, eds., Handbook of Fuel Cells, Wiley, Hoboken, 2009, 91-111.

[70] S. St John, I. Dutta, A.P. Angelopoulos, Synthesis and characterization of electrocatalytically active platinum atom clusters and monodisperse single crystals, Journal of Physical Chemistry C 114(32) (2010) 13515-13525.

[71] F.J. Vidal-Iglesias, Ph.D. thesis, Universidad de Alicante, 2005.

[72] R.E. Davis, G.L. Horvath, C.W. Tobias, The solubility and diffusion coefficient of oxygen in potassium hydroxide solutions, Electrochimica Acta 12(3) (1967) 287-297.

[73] N.R. Elezovic, B.M. Babic, L. Gajic-Krstajic, P. Ercius, V.R. Radmilovic, N.V. Krstajic, L.M. Vracar, Pt supported on nano-tungsten carbide as a beneficial catalyst for the oxygen reduction reaction in alkaline solution, Electrochimica Acta 69 (2012) 239-246.

[74] K. Tammeveski, T. Tenno, J. Claret, C. Ferrater, Electrochemical reduction of oxygen on thin-film Pt electrodes in 0.1 M KOH, Electrochimica Acta 42(5) (1997) 893-897.

[75] N. Alexeyeva, K. Tammeveski, A. Lopez-Cudero, J. Solla-Gullon, J.M. Feliu, Electroreduction of oxygen on Pt nanoparticle/carbon nanotube nanocomposites in acid and alkaline solutions, Electrochimica Acta 55(3) (2010) 794-803.

[76] K. Jukk, J. Kozlova, P. Ritslaid, V. Sammelselg, N. Alexeyeva, K. Tammeveski, Sputter-deposited Pt nanoparticle/multi-walled carbon nanotube composite catalyst for oxygen reduction reaction, Journal of Electroanalytical Chemistry 708 (2013) 31-38.

[77] K. Jukk, N. Kongi, P. Rauwel, L. Matisen, K. Tammeveski, Platinum nanoparticles supported on nitrogen-doped graphene nanosheets as electrocatalysts for oxygen reduction reaction, Electrocatalysis 7(5) (2016) 428-440.

[78] M. Nesselberger, S. Ashton, J.C. Meier, I. Katsounaros, K.J.J. Mayrhofer, M. Arenz, The particle size effect on the oxygen reduction reaction activity of Pt catalysts: Influence of electrolyte and relation to single crystal models, Journal of the American Chemical Society 133(43) (2011) 17428-17433.

[79] I. Katsounaros, S. Cherevko, A.R. Zeradjanin, K.J.J. Mayrhofer, Oxygen electrochemistry as a cornerstone for sustainable energy conversion, Angewandte Chemie International Edition, 53(1) (2014) 102-121.

Figure captions

Figure 1. TEM micrographs of (a) unsupported Pt nanocubes, and carbon-supported cubic Pt nanoparticles: (b) 10, (c) 20, (d) 30, (e) 40 and (f) 50 wt% Pt/C catalysts.

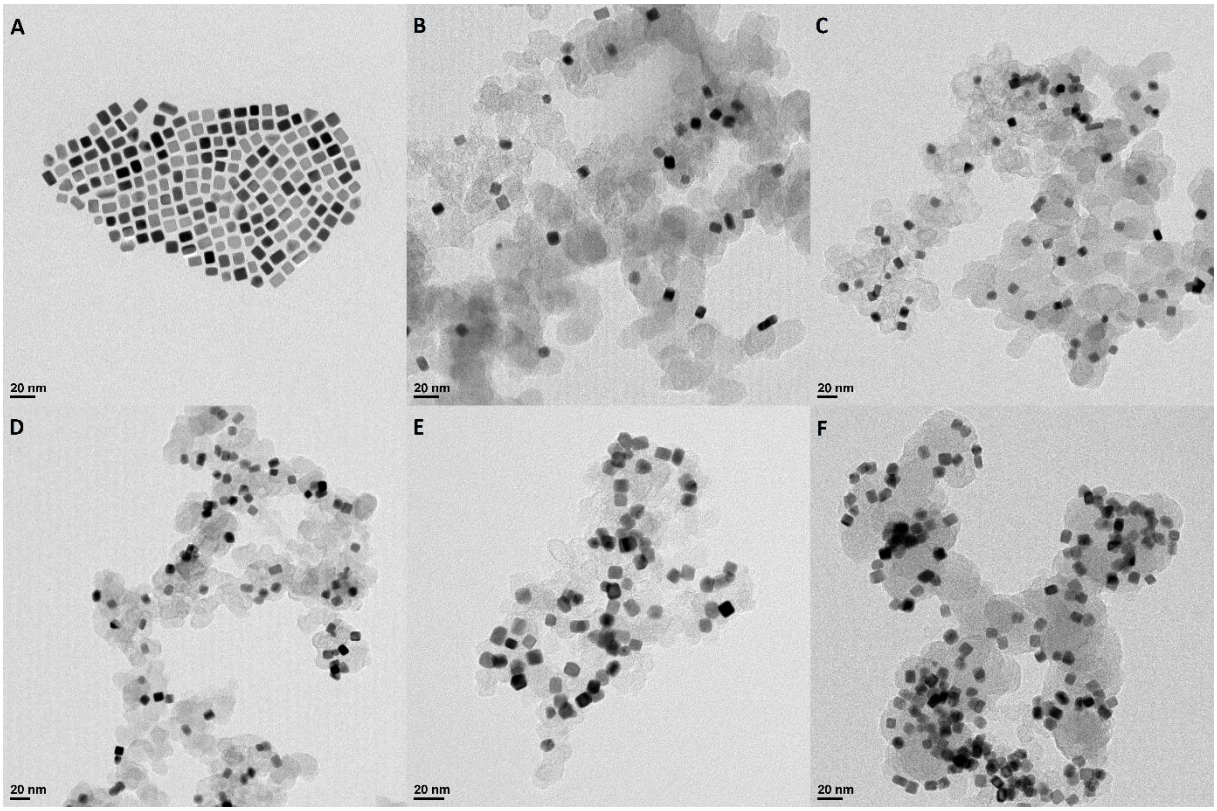

Figure 2. CV curves of (A) unsupported Pt nanoparticles and (B) carbon-supported Pt nanocubes with 10 (magenta), 20 (cyan), 30 (blue), 40 (green) and 50 (red) wt% Pt loading. Test solution: Ar-saturated 0.5 M H_2SO_4, v = 50 mV s^{-1}. Current densities are normalised to the electroactive surface area of Pt.

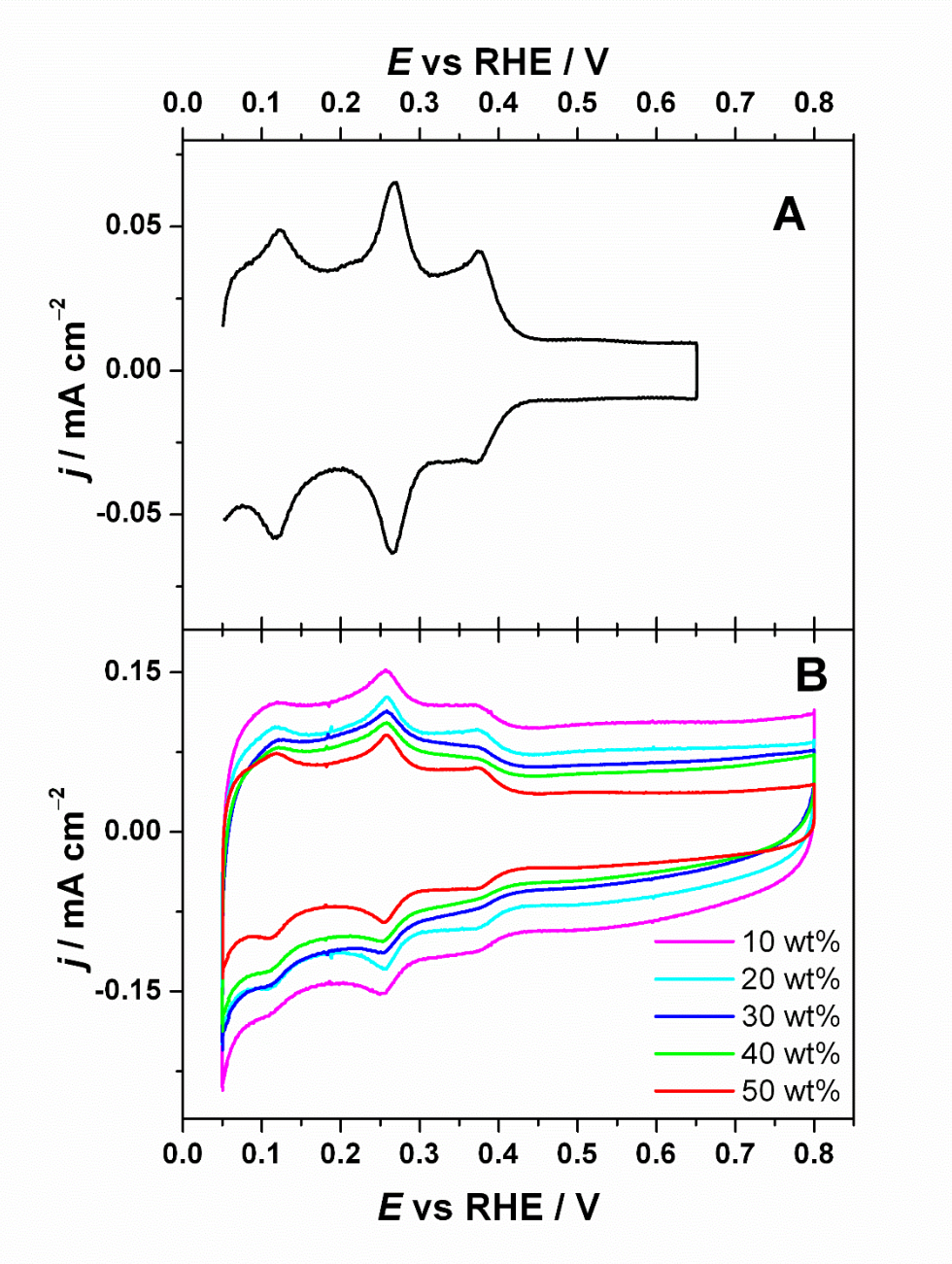

Figure 3. (A) Ratio between current densities at 0.27 V and 0.44 V vs RHE for each sample vs the Pt loading. (B) A_r vs Pt loading. The linear fit is also presented in both cases. Test solution: Ar-saturated 0.5 M H_2SO_4, v = 50 mV s^{-1}.

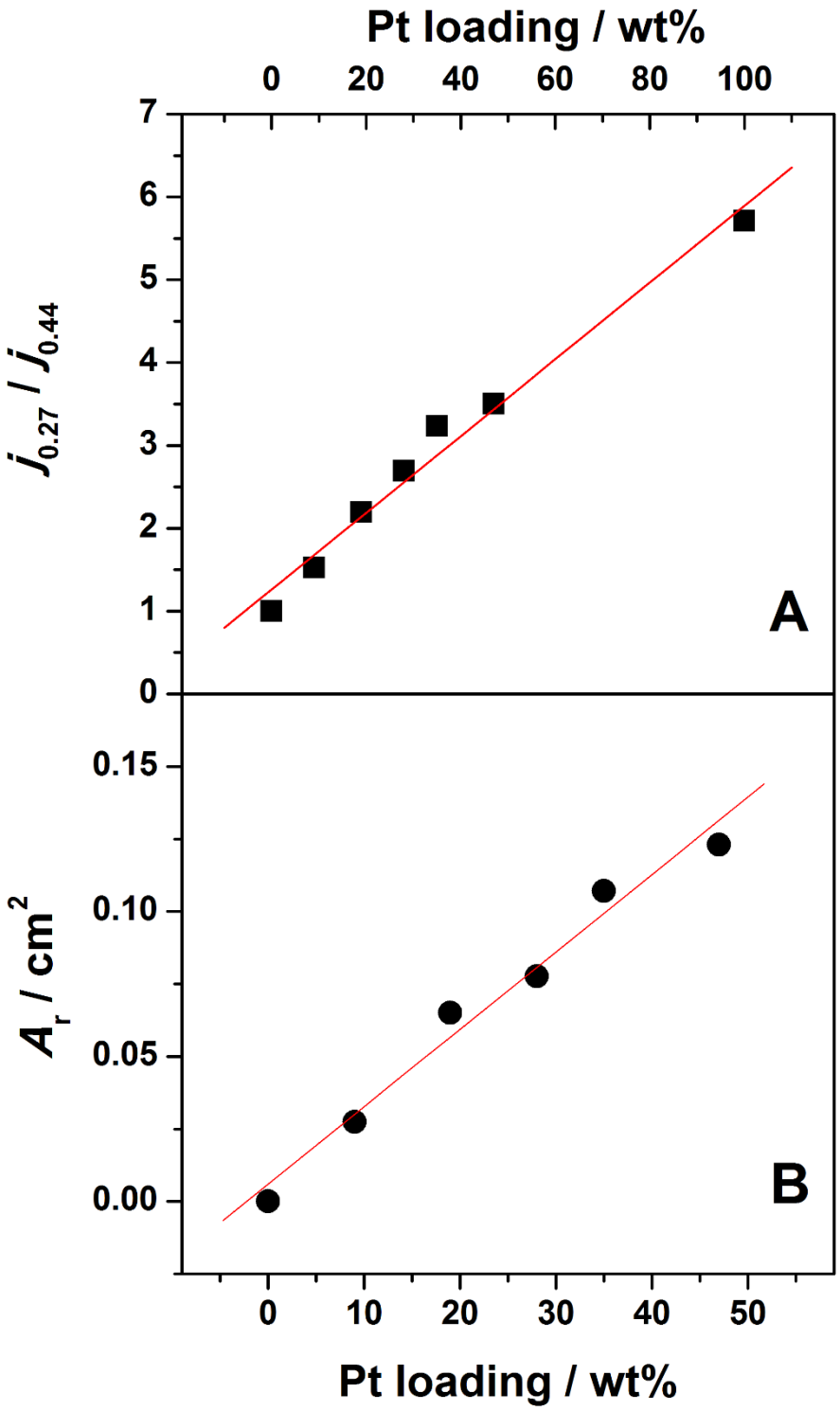

Figure 4. CV curves of (A) unsupported Pt nanoparticles and (B) carbon-supported Pt nanocubes with 10 (magenta), 20 (cyan), 30 (blue), 40 (green) and 50 (red) wt% Pt loading. Test solution: Ar-saturated 0.1 M $HClO_4$, v = 50 mV s^{-1}. (C) A_r vs Pt loading. The linear fit is also presented.

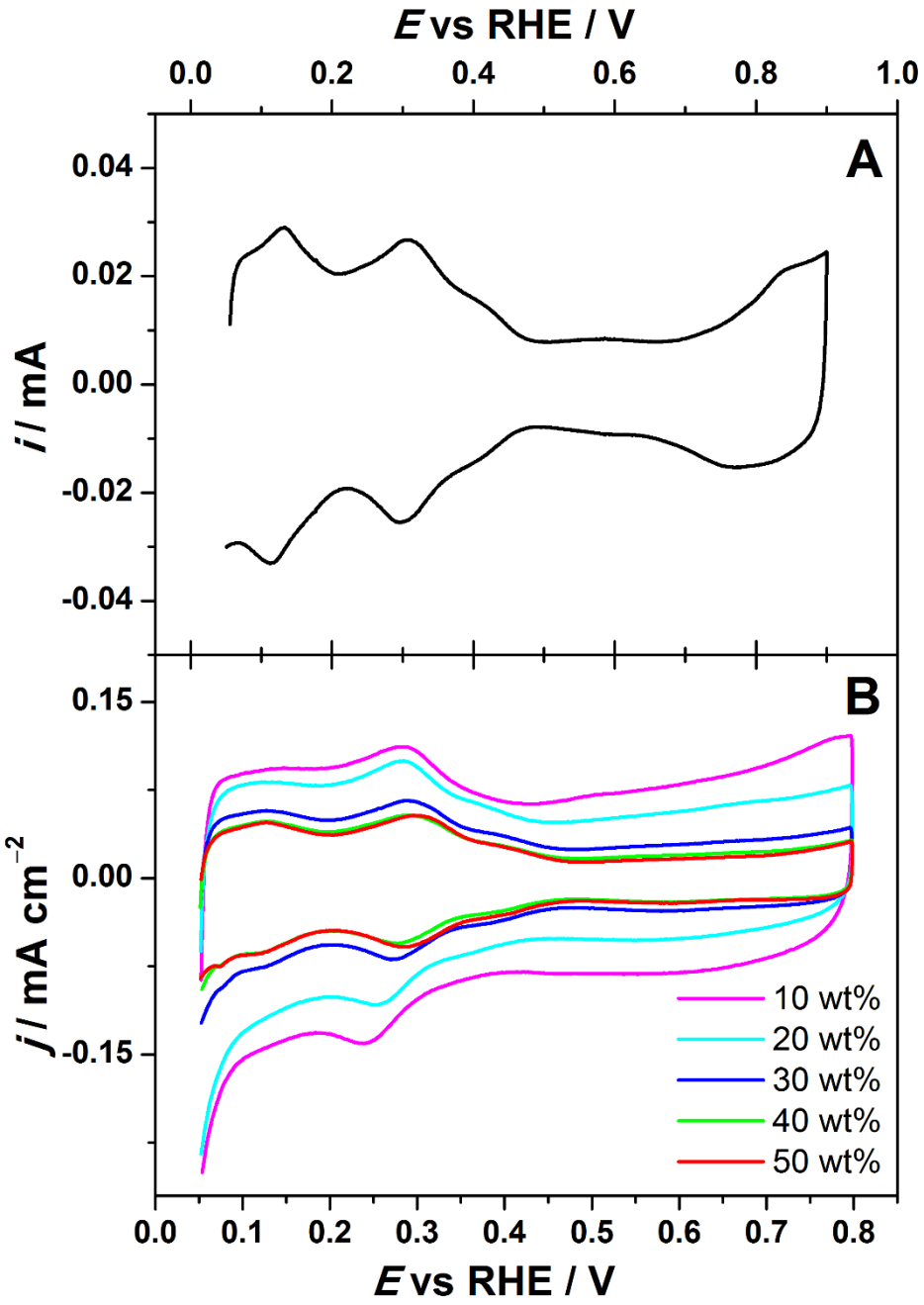

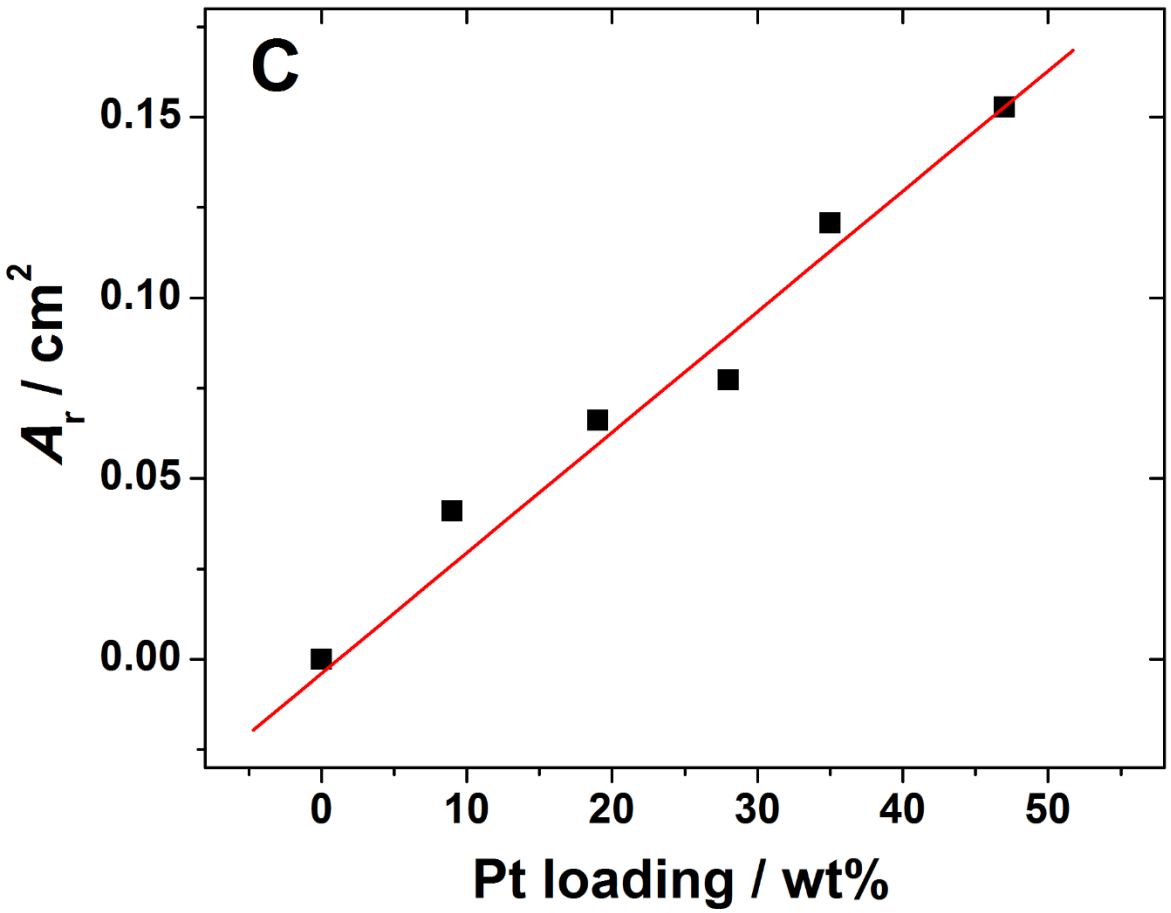

Figure 5. (A) ORR polarisation curves for a 30% Pt/C catalyst in O_2-saturated 0.1 M $HClO_4$ at different rotation rates (v = 10 mV s^{-1}), (B) the corresponding K-L plots in 0.1 M $HClO_4$ (inset shows n dependence on potential), (C) comparison of the RDE results of Pt/C modified GC electrodes in O_2-saturated 0.1 M $HClO_4$ at 1900 rpm (v = 10 mV s^{-1}), (D) Tafel plots for O_2 reduction in 0.1 M $HClO_4$ (ω = 1900 rpm). Current densities are normalised to the geometric area of GC.

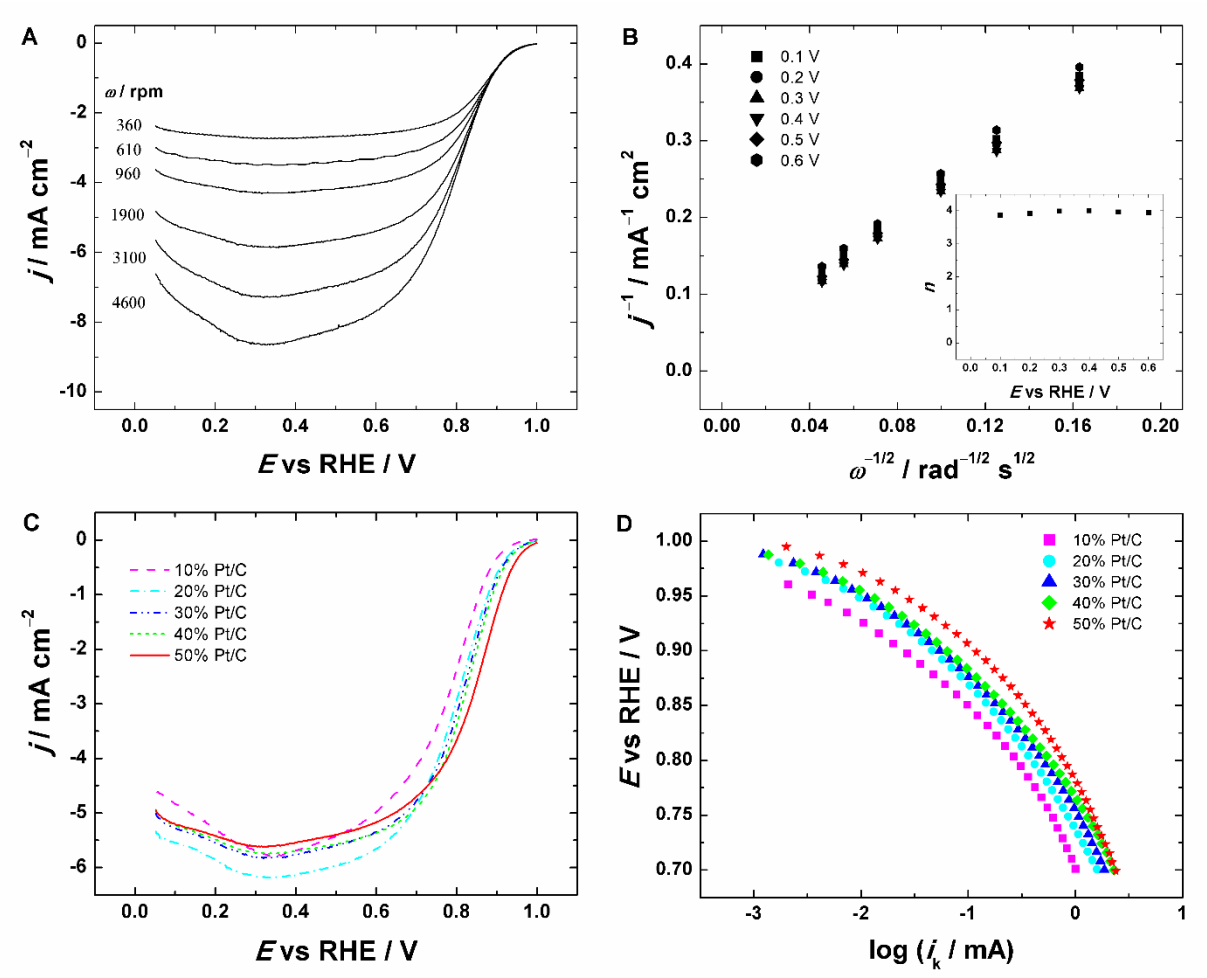

Figure 6. The dependence of (A) specific activity and (B) mass activity for O_2 reduction on the Pt loading in O_2-saturated 0.1 M $HClO_4$ solution at 0.9 V vs RHE. The SA and MA values are mean values calculated from at least 3-4 independent measurements.

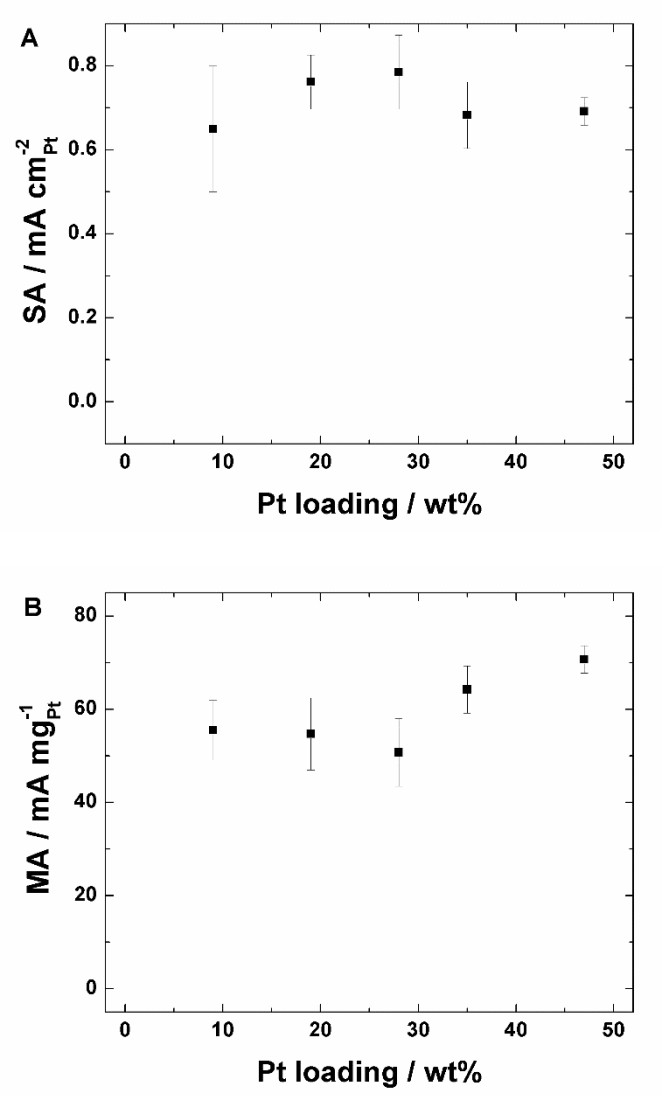

Figure 7. (A) CV curves of carbon-supported cubic Pt nanoparticles with 10 (magenta), 20 (cyan), 30 (blue), 40 (green) and 50 (red) wt% Pt loading. (B) Region used for the calculation of the electroactive surface area. Test solution: Ar-saturated 0.1 M KOH, v = 50 mV s^{-1} (C) A_r vs Pt loading. The linear fit is also presented.

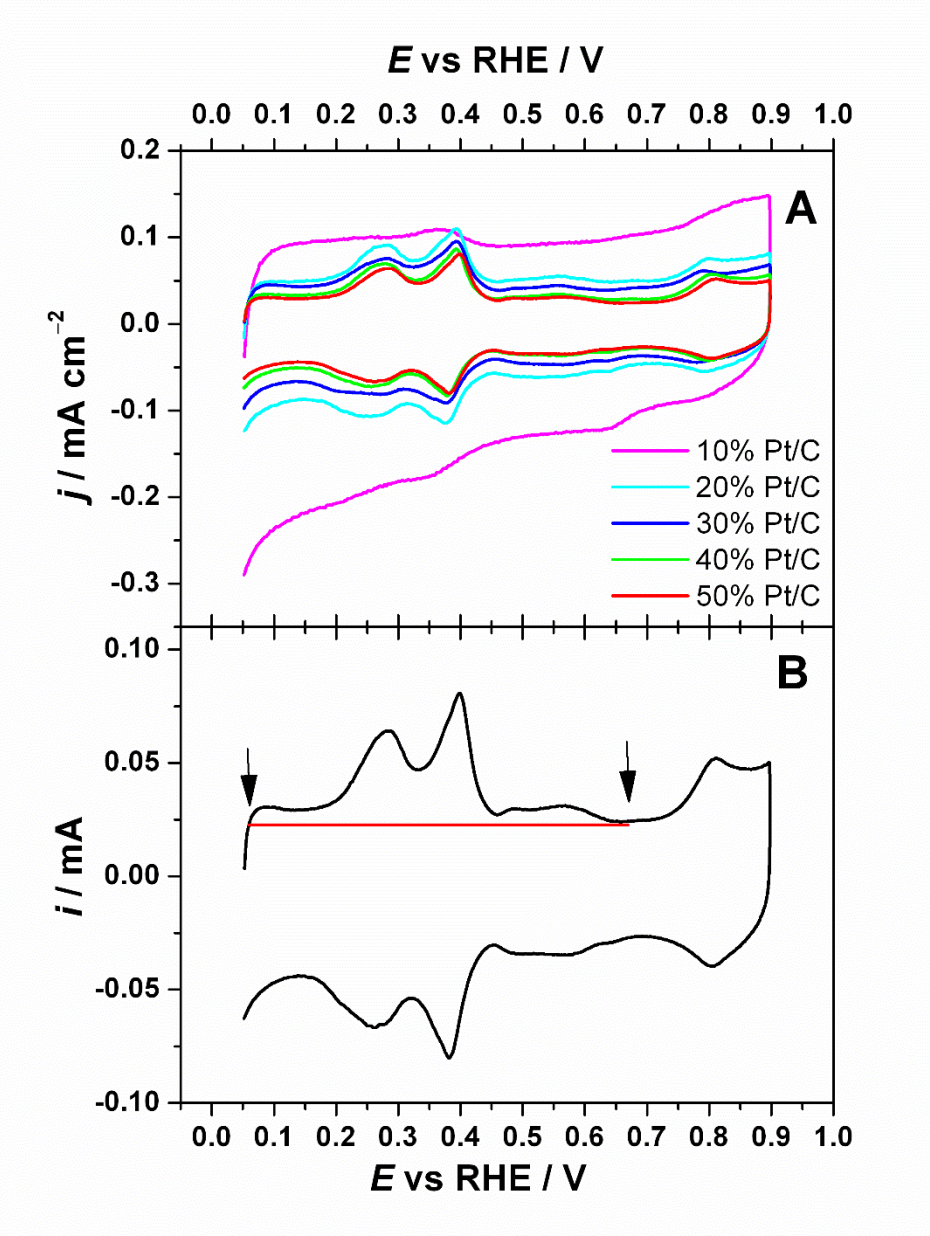

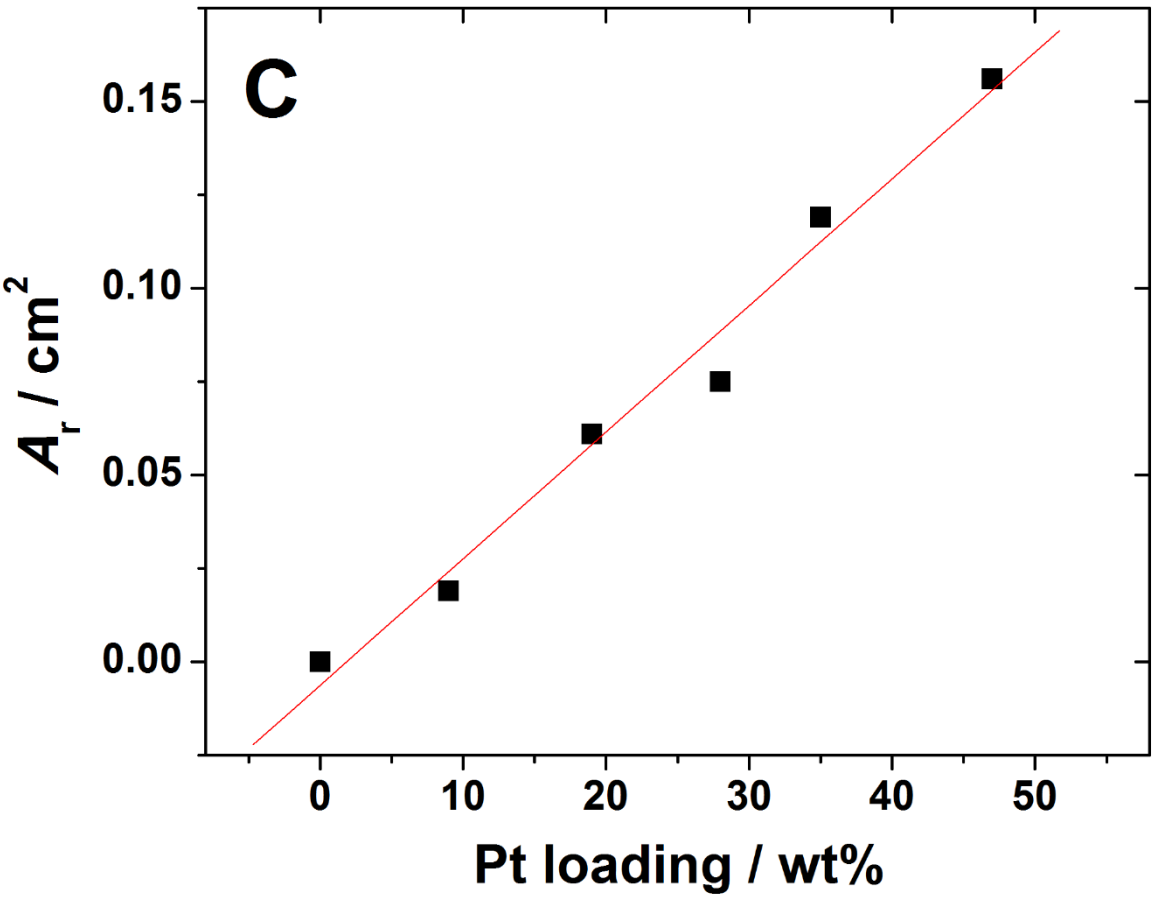

Figure 8. (A) ORR polarisation curves for a 30% Pt/C catalyst in O_2-saturated 0.1 M KOH at different rotation rates (v = 10 mV s^{-1}), (B) the corresponding K-L plots in 0.1 M KOH (inset shows n dependence on potential), (C) comparison of the RDE results of Pt/C modified GC electrodes in O_2-saturated 0.1 M KOH at 1900 rpm (v = 10 mV s^{-1}), (D) Tafel plots for O_2 reduction in 0.1 M KOH (ω = 1900 rpm). Current densities are normalised to the geometric area of GC.

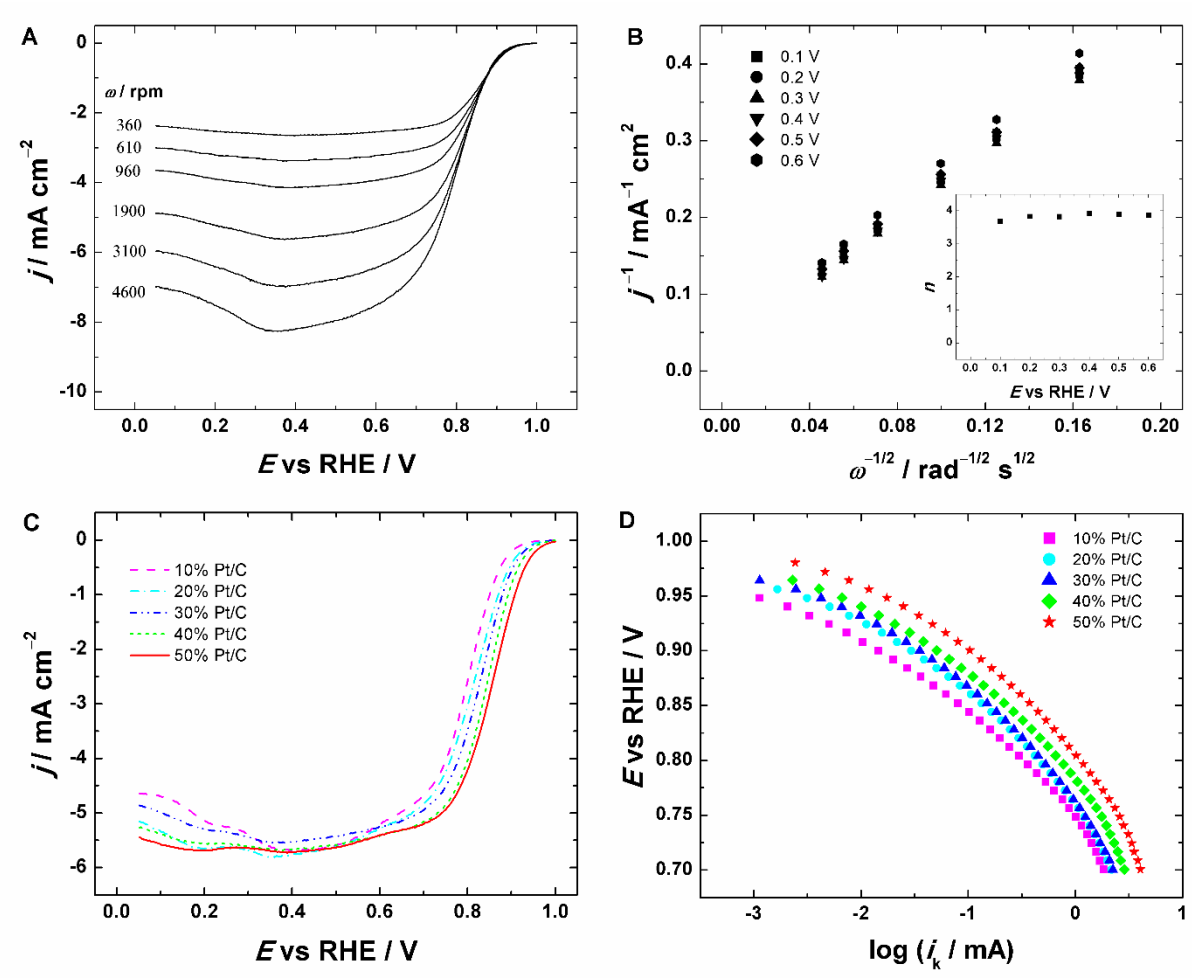

Figure 9. The dependence of (A) specific activity and (B) mass activity for O_2 reduction on the Pt loading in O_2-saturated 0.1 M KOH solution at 0.9 V vs RHE. The SA and MA values are mean values calculated from at least 3-4 independent measurements.

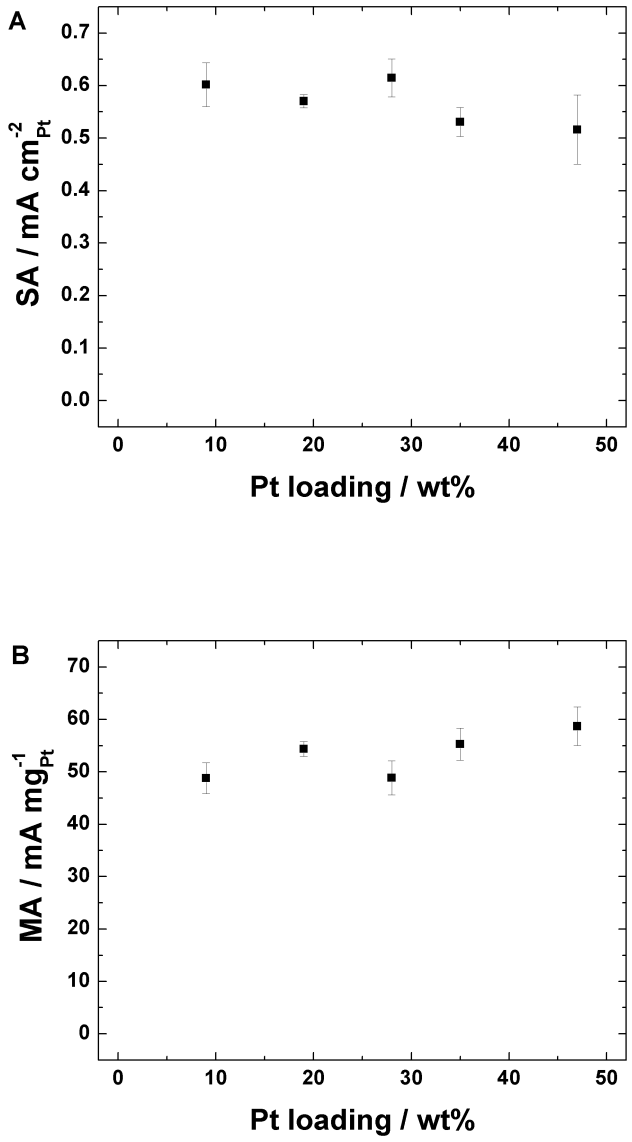

Table 1. Kinetic parameters for oxygen reduction on Pt/C modified GC electrodes in O_2-saturated 0.1 M $HClO_4$ and 0.1 M KOH solutions (v = 10 mV s^{-1}, ω = 1900 rpm).

Electrode	A_r (cm^2)	Tafel slope (V) I region*	Tafel slope (V) II region*	$E_{1/2}$ (V)	A_r (cm^2)	Tafel slope (V) I region*	Tafel slope (V) II region*	$E_{1/2}$ (V)
	0.1 M $HClO_4$				0.1 M KOH			
10% Pt/C	0.041	-0.062	-0.117	0.78	0.019	-0.061	-0.114	0.79
20% Pt/C	0.066	-0.064	-0.126	0.79	0.061	-0.064	-0.127	0.80
30% Pt/C	0.077	-0.065	-0.128	0.81	0.075	-0.063	-0.128	0.82
40% Pt/C	0.121	-0.063	-0.126	0.82	0.119	-0.062	-0.128	0.84
50% Pt/C	0.153	-0.063	-0.125	0.85	0.156	-0.064	-0.134	0.85

* Region I corresponds to low current densities and Region II to high current densities.